Metallophysics and Advanced Technologies
Металофіз. новітні технол.
Metallofiz. Noveishie Tekhnol.
2024, vol. 46, No. 9, pp. 881–891
https://doi.org/10.15407/mfint.46.09.0881
Reprints available directly from the publisher

PACS numbers: 61.66.Dk, 61.72.Ff, 62.20.Qp, 64.75.Nx, 81.30.Mh, 81.40.Cd, 81.40.Ef

Increasing the Operating Temperatures of High-Strength Wrought Al–Zn–Mg–Cu Alloys by Means of Doping with Transition Metals

M. O. Iefimov, N. P. Zakharova, M. I. Danylenko, and K. O. Iefimova

I. M. Frantsevich Institute for Problems in Materials Science, N.A.S. of Ukraine,
3 Omeljan Pritsak Str.,
UA-03142 Kyiv, Ukraine

The effect of doping with scandium, zirconium, and hafnium on the thermal stability of high-strength wrought Al–Zn–Mg–Cu (of 7XXX series) alloys at 80°C for 100 hours is investigated. The study is performed on rods produced by a two-stage hot extrusion of 1500 g ingots. As shown, the doping with scandium and zirconium has improved the hardness and strength characteristics due to the occurrence of two ensembles of dispersed precipitates: intermetallics η′-phase ($MgZn_2$) and $Al_3(Sc_{1-x}Zr_x)$ particles coherently bonded with the aluminium matrix. As proved, in the 7XXX alloy, which is additionally doped with the (Sc + Zr + Hf) complex, the composition of nanosize precipitates based on Al_3Sc intermetallic compound includes zirconium and hafnium. The alloying of the base alloy with the complex (Sc + Zr + Hf) stabilizes the structural state of the alloy and, after holding at 80°C, no significant changes in the size and distribution of strengthening particles are observed. This makes it possible to obtain high strength characteristics of Al–Zn–Mg–Cu alloys with a high level of plasticity at long-term holding at 80°C.

Key words: aluminium alloys, additional doping, scandium, zirconium, hafnium, mechanical properties.

Досліджено вплив леґування Скандієм, Цирконієм і Гафнієм на термічну стабільність високоміцних деформівних стопів системи Al–Zn–Mg–Cu за витримки при 80°C упродовж 100 годин. Дослідження виконано на прутках, яких було одержано методом двоступеневої гарячої екструзії вилив-

Corresponding author: Mykola Oleksandrovych Iefimov
E-mail: n.iefimov@gmail.ua

Citation: M. O. Iefimov, N. P. Zakharova, M. I. Danylenko, and K. O. Iefimova, Increasing the Operating Temperatures of High-Strength Wrought Al–Zn–Mg–Cu Alloys by Means of Doping with Transition Metals, *Metallofiz. Noveishie Tekhnol.*, **46**, No. 9: 881–891 (2024). DOI: 10.15407/mfint.46.09.0881

ків вагою у 1500 г. Показано, що завдяки леґуванню Скандієм і Цирконієм досягнуто підвищення характеристик твердости та міцности за рахунок наявности двох ансамблів дисперсних зміцнювальних частинок: інтерметалідів η′-фази ($MgZn_2$) та когерентно пов'язаних із матрицею частинок $Al_3(Sc_{1-x}Zr_x)$. Доведено, що у стопі на основі системи Al–Zn–Mg–Cu, який додатково було леґовано комплексом (Sc + Zr + Hf), до складу нанорозмірних зміцнювальних частинок на основі інтерметаліду Al_3Sc також входять Цирконій і Гафній. Леґування базового стопу комплексом (Sc + Zr + Hf) стабілізує структурний стан стопу, а після витримки при 80°C не фіксується значних змін у розмірі та розподілі зміцнювальних частинок η′-фази ($MgZn_2$) і $Al_3(Sc_{1-x-y}Zr_xHf_y)$, що дає змогу одержати високий рівень механічних властивостей зі збереженням високого рівня пластичности за довготривалої витримки при 80°C.

Ключові слова: алюмінійові стопи, додаткове леґування, Скандій, Цирконій, Гафній, механічні властивості.

(Received 9 July, 2024; in final version, 12 July, 2024)

1. INTRODUCTION

The ever-increasing demands on aircraft structures due to growth in size, speed, durability, reliability and efficiency have somewhat changed a number of requirements for high-strength alloys, including aluminium alloys used in aircraft and aircraft engines.

Currently, many research centres in the United States and Europe are conducting intensive research aimed at developing high-strength aluminium alloys that can replace titanium alloys in aircraft engine construction, thereby reducing their weight and simplifying the manufacturing process. In particular, the development of aluminium alloys with a tensile strength of at least 600 MPa at 80°C is relevant for the manufacture of external fan blades for aircraft gas turbine engines.

Currently, alloys based on the Al–Zn–Mg–Cu system (of 7XXX series) have the highest strength among wrought aluminium alloys (up to 700–800 MPa) [1].

In wrought Al–Zn–Mg–Cu alloys, the strength after heat treatment is mainly determined by the content of zinc and magnesium, which, among all other alloying components, are characterized by the highest solubility in aluminium at elevated temperatures. The solubility of these elements decreases sharply during cooling, which causes significant hardening of the alloy as a result of both quenching and ageing [2]. Copper in commercial alloys of the Al–Zn–Mg–Cu system significantly increases the hardening effect by alloying of aluminium solid solution, but has little effect on the ageing [3]. With copper content up to 2% wt. and zinc in the range of 5–10% wt., copper is in a supersaturated solid solution and has a beneficial effect on the whole complex of

properties, causing an increase in strength, ductility, effective increase in stress corrosion resistance and durability. Copper also increases the resistance to crack growth in fatigue tests.

However, a major disadvantage of 7XXX alloys is their low working temperature, which is due to a sharp increase in the rate of diffusion processes in aluminium alloys with a high Zn content.

One of the promising directions for further improving the physical, mechanical, and operational characteristics of modern aluminium alloys of the Al–Zn–Mg–Cu system is their complex alloying with scandium and other transition metals, since the diffusion coefficients in solid aluminium, which is a criterion for the diffusion interaction of the strengthening phase with the matrix, are several orders of magnitude lower for transition metals than for Zn, Cu and Mg [4].

It has been previously shown that one of the most effective hardening and antirecrystallization components for 7XXX alloys is scandium [4–7].

A significant increase in strength and satisfactory ductility in Sc alloyed aluminium alloys is possible due to the precipitation of secondary Al_3Sc particles, which causes the highest specific strengthening of the aluminium matrix compared to all elements of the periodic system and promotes the formation of a fine, uniform cellular structure that increases thermal stability.

Alloying with scandium dramatically increases the recrystallization temperature of aluminium alloys; the efficiency of scandium as an antirecrystallizer is significantly higher than that of other transition metals such as Mn, Cr, Zr, V, Ti, *etc*. Scandium retains excess vacancies in the alloy matrix, forming complexes that prevent the release of alloying elements to the grain boundaries. In addition, scandium significantly reduces the anisotropy of the mechanical properties of pressed and rolled semi-finished products of highly alloyed aluminium alloys.

Doping of Al–Zn–Mg–Cu–Sc alloys with zirconium contributes to the thermal stabilization of Al_3Sc particles. In particular, work [5] shows that the simultaneous alloying with Zr and Sc replaces some of the scandium atoms within the Al_3Sc particles with Zr atoms. By the properties, the $Al_3(Sc_{1-x}Zr_x)$ phase is very close to the Al_3Sc phase, but is characterized by a much lower ability to coagulate when heated.

As has been shown, Hf slightly increases the hardening and antirecrystallization effect in Al–Zn–Mg–Cu alloys [8].

The efficiency of scandium alloying of aluminium alloys can be significantly improved by increasing the cooling rate during ingot crystallization to create a supersaturated solid solution of aluminium [9, 10].

The aim of this work is to study the effect of additional alloying with Sc, Zr, and Hf of wrought Al–Zn–Mg–Cu alloys on their structure and mechanical properties at 80°C.

2. EXPERIMENTAL DETAILS

To improve the mechanical properties of the alloy of the base composition Al–8.0Zn–2.6Mg–2.3Cu, additional microalloying with the complex (Sc + Zr) was used and the effect of hafnium Hf on the stability of mechanical properties during prolonged holding at 80°C was studied. The chemical composition of the experimental alloys is given in Table 1.

Semi-finished products were made from the investigated ingots by extrusion. To improve the cast structure, two-stage extrusion was used: from ∅ 55 mm to ∅ 25 mm and from ∅ 25 mm to ∅ 6 mm (total elongation ∅ = 58). Before that, the samples were ground to remove surface defects.

When extruding ingots from ∅ 55 mm to ∅ 25 mm, electrically heated moulds were used to stabilize the temperature during the deformation process. Ingots were heated in an electric furnace. Ingot heating was controlled by thermocouples placed in the heating zone. The heating temperature of ingots and mould was 350°C. The holding time of ingots in the electric furnace was 50 min. The pressure force during ingot extrusion varied from 0.85 to 1.25 MN, depending on the ingot composition. Samples from ∅ 25 mm to ∅ 6 mm were extruded using moulds that were heated in an electric furnace together with the samples. The heating time was of 30 min.

The samples of the test alloys obtained after hot extrusion were processed according to the T6 maintenance regime, namely, water quenching from 465°C + annealing 120°C for 24 hours.

The chemical analysis of the obtained alloys was performed by x-ray fluorescence analysis.

The structure of the samples was studied by transmission electron microscopy (TEM), using a JEM-100CX microscope and a JEM-2100F high-resolution microscope.

The hardness of the obtained samples was measured using a Vickers IT50/10 hardness tester with a load of 100 N. Mechanical tensile tests of the deformed bars were performed on a 1246 testing machine with a gripper movement speed of 1 mm/min (strain rate of about 10^{-3} s^{-1} with a strain curve recorded). The tensile strength U_{TS}, yield strength Y_S, and elongation to failure E_l [%] were calculated from the strain curves.

TABLE 1. Chemical composition of the investigated Al–Zn–Mg–Cu alloys.

Nos. alloys	Chemical composition, % wt.
1	Al–8.0Zn–2.6Mg–2.3Cu
2	Al–8.0Zn–2.6Mg–2.3Cu–0.15Zr–0.3Sc
3	Al–8.0Zn–2.6Mg–2.3Cu–0.15Zr–0.3Sc–0.2Hf

3. RESULTS AND DISCUSSION

The study of the structure of extruded rods of 7XXX alloys after T6 treatment is shown in Figs. 1–4. After T6, large recrystallized grains with an average size of 8–9 μm are formed in the base alloy.

It is generally recognized [11–13] that, depending on the concentration of zinc, the eutectic layers of Al–Zn–Mg–Cu alloys contain nanosized precipitates of the η′-phase ($MgZn_2$) and/or T-phase $Mg_3Zn_3Al_2$. Precipitation hardening provides high mechanical properties of Al–Zn–Mg–Cu alloys during quenching and subsequent ageing. The η′-phase is formed when the ratio of atomic concentrations of $Zn/Mg > 2$. In the case of $Zn/Mg < 2$, the T-phase prevails. At the same time, copper is almost completely dissolved in these phases if the ratio of atomic concentrations of $Cu/Mg < 1$. In the alloy Al–8.0Zn–2.6Mg–2.3Cu, $Zn/Mg > 2$ and $Cu/Mg \approx 0.88$, therefore, the η′-phase ($MgZn_2$) prevails in the alloys of the studied composition. Particles of the η′-phase are located mainly along the grain boundaries but sometimes they can be observed inside the grains.

A cellular structure is observed in the extruded alloy alloyed with the (Sc + Zr) complex after T6 heat treatment (Fig. 2, *a*). The average cell size is of 1.0–1.5 μm. From the dark field image in the η′-phase diffraction spot (Fig. 2, *b*), it can be concluded that there are hardening particles of different sizes in the bar structure. The average size of the strengthening particles of the η′-phase is of 5–6 nm). Secondary precipitates of the Al_3Sc type in TEM bright images have a characteristic two-lobe Ashby–Brown contrast, which is typical for coherent precipitates [14]. The dark field image in the Al_3Sc diffraction spot is shown in Fig. 2, *c*. The average size of these particles reaches 15–20 nm.

A cellular structure is also formed in extruded sample from the alloy adopted with a complex (Sc + Zr + Hf) after T6 treatment, with strengthening phases observed both in the body and at the cell boundaries.

The average cell size is of 0.9–1.1 μm (Fig. 3, *a*). The average particle size of the η′-phase is of 5–6 nm (Fig. 3, *b*). Based on the dark field image obtained from the $Al_3(Sc_{1-x}Zr_x)$ diffraction spot, the average size of these particles is of 15–20 μm (Fig. 3, *c*).

A high-resolution electron microscope JEOL-100CX was used to analyse the hardening particles of Al_3Sc in extruded samples from Al–8.0Zn–2.6Mg–2.3Cu–0.3Sc–0.2Cr–0.1Zr–0.1Hf alloy after T6 treatment (Fig. 4). Chemical micro-x-ray spectral analysis showed that the composition of these particles includes both Sc and Zr and Hf (Table 2).Thus, in the alloy alloyed with Sc, Zr and Hf, the composition of the strengthening particles can be described as $Al_3(Sc_{1-x-y}Zr_xHf_y)$.

The hardness of the extruded rods from the investigated alloys after T6 treatment at room temperature and after holding at 80°C for 100 hours is given in Table 3.

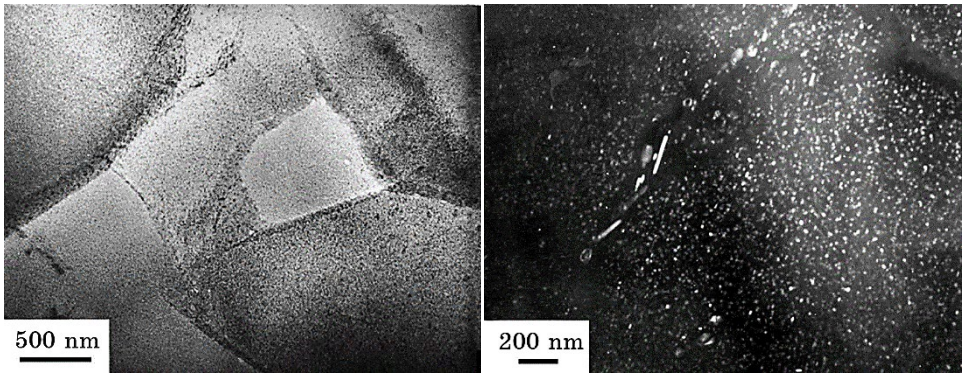

Fig. 1. TEM images of Al–8.0Zn–2.6Mg–2.3Cu hot extruded samples: bright field (*a*), dark field obtained from the η′-phase diffraction spot (*b*).

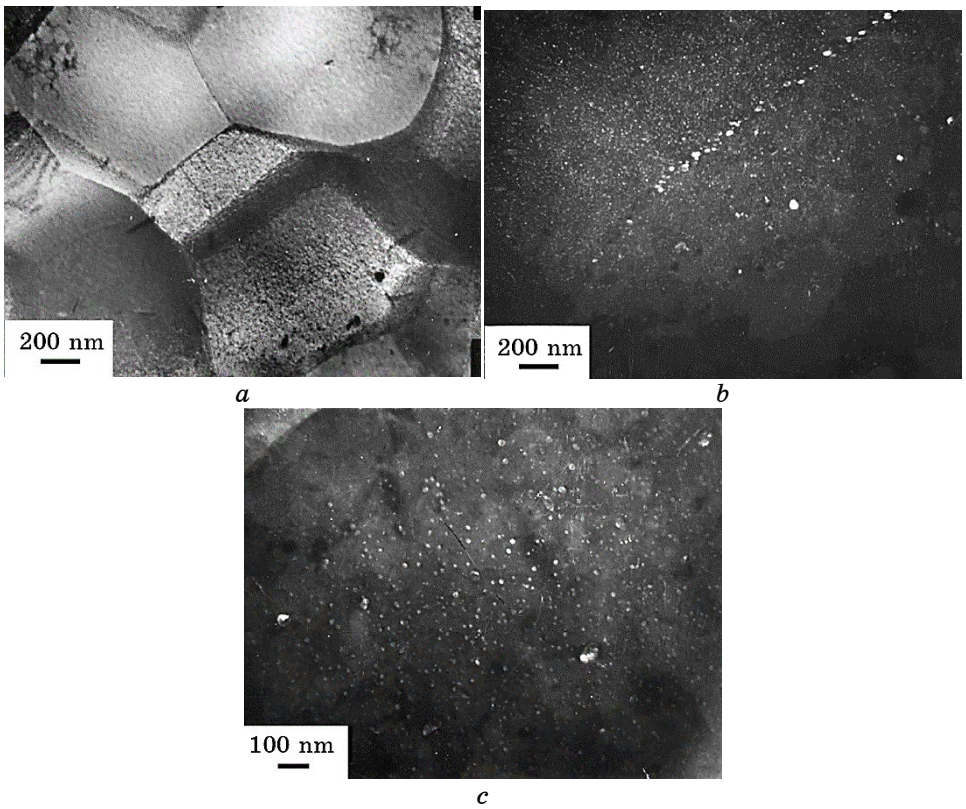

Fig. 2. TEM images of Al–8.0Zn–2.6Mg–2.3Cu–0.15Zr–0.3Sc hot extruded samples: bright field (*a*), dark field obtained from the η′-phase diffraction spot (*b*), dark field obtained from the Al_3Sc diffraction spot (*c*).

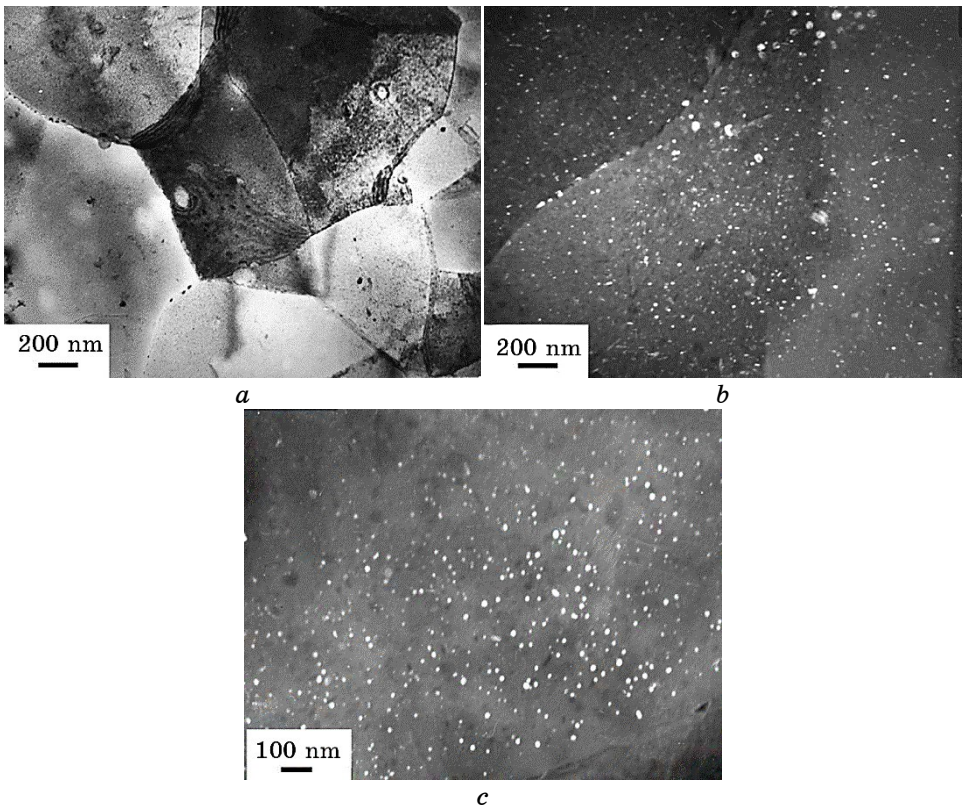

Fig. 3. TEM images of Al–8.0Zn–2.6Mg–2.3Cu–0.15Zr–0.3Sc–0.2Hf hot extruded samples: bright field (*a*), dark field obtained from the η′-phase diffraction spot (*b*), dark field obtained from the Al_3Sc diffraction spot (*c*).

The data of mechanical tests of the rods from the investigated Al–Zn–Mg–Cu alloys at room temperature and 80°C are given in Table 4.

The strain curves of the alloys after testing showed a slight strain-hardening characteristic of highly hardened materials. The increase in hardness and strength characteristics of the investigated alloys after holding at 80°C indicates the continuation of ageing processes at this temperature.

The analysis of mechanical test data proves that the selected system of additional alloying with the (Sc + Zr) complex allows obtaining a higher level of mechanical properties during tests at 80°C for 100 hours. The addition of 0.2% wt. Hf to the (Sc + Zr) complex allows improving the mechanical properties of the investigated alloy after holding for 100 hours at 80°C. In addition, the alloying of the base composition with the (Sc + Zr + Hf) complex provides an increase in ductility both at room temperature and 80°C.

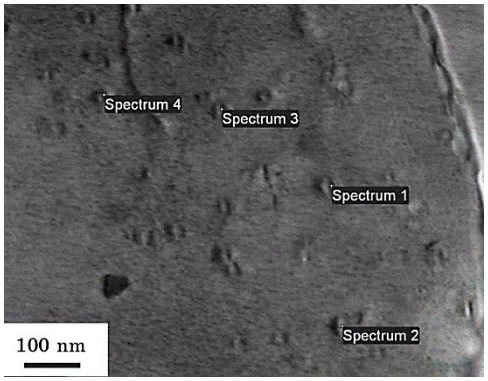

Fig. 4. Bright field TEM images of secondary particles of Al_3Sc-based intermetallics in the structure of the alloy Al–8.0Zn–2.6Mg–2.3Cu–0.3Sc–0.2Cr–0.1Zr–0.1Hf.

TABLE 2. Chemical analysis of the structural components in Fig. 4 in the alloy Al–8.0Zn–2.6Mg–2.3Cu–0.3Sc–0.2Cr–0.1Zr–0.1Hf.

Spectrum	Content of chemical elements, % wt.							
	Mg	Al	Sc	Cu	Zn	Zr	Hf	Mg
Spectrum 1	1.78	91.52	0.73	2.26	3.26	0.19	0.18	1.78
Spectrum 2	1.90	90.83	1.23	2.49	3.11	0.13	0.23	1.90
Spectrum 3	2.39	90.86	0.61	2.40	3.39	0.06	0.10	2.39
Spectrum 4	1.82	91.81	0.41	2.49	3.11	0.01	0.18	1.82

Structural changes in the rods from the investigated Al–Zn–Mg–Cu alloys after T6 treatment can be explained on the basis of the analysis of dark field images obtained from the η′ and Al_3Sc diffraction spot.

Thus, the increase in the level of hardness and strength characteristics of the studied alloys after holding the bars at 80°C for 100 hours is explained by the further ageing processes at a temperature of 80°C (Figs. 5, 6). It is noticeable that after holding the base unalloyed alloy at 80°C for 100 hours, an increase in the particle size of the η′-phase (Fig. 5, *b*) is observed compared to the alloy state after T6 (Fig. 5, *a*). Such processes lead to a deterioration in the thermal stability of Al–Zn–Mg–Cu alloys at long-term exposures at 80°C and reduce the level of the complex of mechanical properties.

The doping of the base alloy with the (Sc + Zr) complex and the (Sc + Zr + Hf) complex stabilizes the structure, and, at 80°C, no significant changes in the size and distribution of strengthening particles of both types are observed (Fig. 6). The dark field images in the η′-phase reflexes before and after ageing at 80°C show that the size of this phase remains unchanged (Fig. 6, *a*, *b*).

TABLE 3. Hardness of extruded rods from the investigated Al–Zn–Mg–Cu alloys after T6 treatment and after T6 heat treatment + holding at 80°C for 100 hours.

No. alloy	Chemical composition, % wt.	*HV*, MPa	
		T6 treatment	T6 treatment + holding at 80°C for 100 hours
1	Al–8.0Zn–2.6Mg–2.3Cu	1880	1970
2	Al–8.0Zn–2.6Mg–2.3Cu–0.15Zr–0.3Sc	2010	2070
3	Al–8.0Zn–2.6Mg–2.3Cu–0.15Zr–0.3Sc–0.2Hf	2030	2270

TABLE 4. Mechanical properties of rods from the investigated Al–Zn–Mg–Cu alloys after T6 treatment (tensile strength at room temperature and at 80°C).

No. alloy	Tensile tests at room temperature			Tensile tests at 80°C			Tensile tests at 80°C after holding at 80°C for 100 hours		
	Y_S, MPa	U_{TS}, MPa	E_l, %	Y_S, MPa	U_{TS}, MPa	E_l, %	Y_S, MPa	U_{TS}, MPa	E_l, %
1	530	619	13.2	542	556	19.6	512	564	14.5
2	674	775	6.4	620	670	9.8	630	705	10.0
3	737	776	13.6	611	725	16.4	636	731	14.5

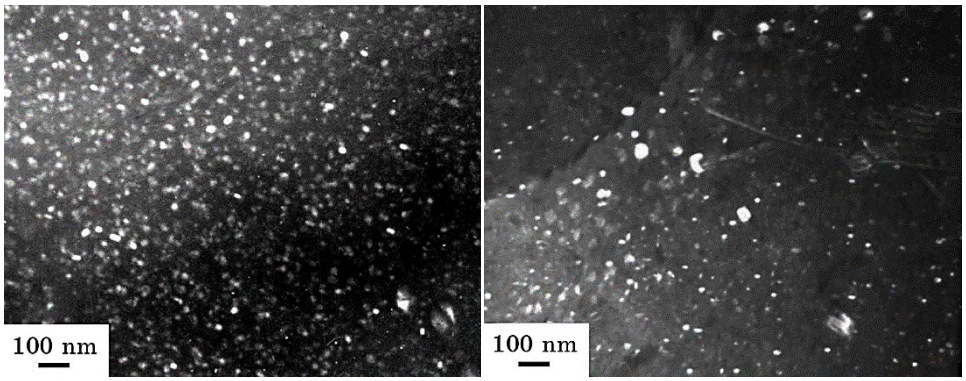

Fig. 5. TEM images of Al–8.0Zn–2.6Mg–2.3Cu hot extruded samples, dark field image obtained from the η′-phase diffraction spot: T6 treatment (*a*), T6 treatment + holding at 80°C for 100 hours (*b*).

At the same time, the number of η′-phase particles slightly increases due to the continued ageing process. The dark field images in Al_3Sc re-

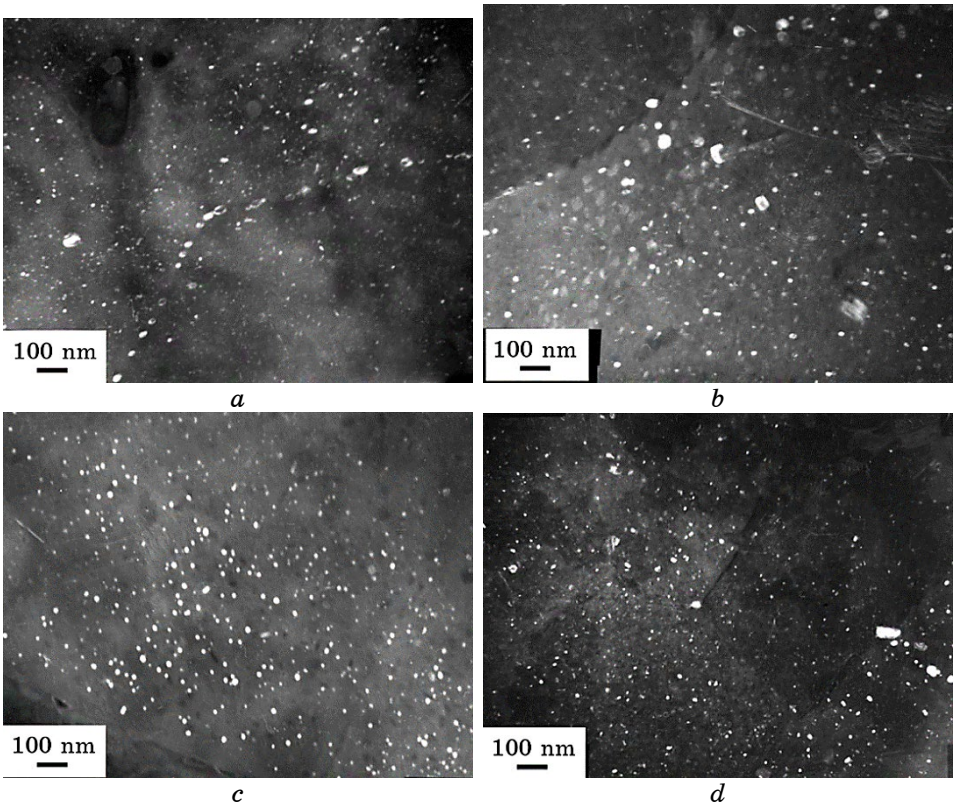

Fig. 6. TEM images of Al–8.0Zn–2.6Mg–2.3Cu–0.15Zr–0.3Sc–0.2Hf hot extruded samples: dark field image obtained from the η′-phase diffraction spot, T6 treatment (*a*), dark field image obtained from the η′-phase diffraction spot, T6 treatment + holding at 80°C for 100 hours (*b*), dark field image obtained from the Al_3Sc diffraction spot, T6 treatment (*c*), dark field image obtained from the Al_3Sc diffraction spot, T6 treatment + holding at 80°C for 100 hours (*d*).

flexes confirm the stability of the size of these particles after ageing at 80°C (Fig. 6, *c*, *d*).

Thus, the coherent bonds of $Al_3(Sc_{1-x-y}Zr_xHf_y)$ particles with the matrix and the resulting internal stresses exclude the growth of the η′-phase, which in turn increases the mechanical properties and thermal stability of alloyed Al–Zn–Mg–Cu alloys.

The obtained results are consistent with the theoretical concepts of diffusion processes in dispersion-strengthened alloys [15].

4. CONCLUSION

1. The effectiveness of a combined doping of aluminium alloys of the

Al–Zn–Mg–Cu system with scandium, zirconium and hafnium is demonstrated.

2. It is shown that doping of Al–Zn–Mg–Cu alloys with Sc and Zr results in an improvement of investigated hardness and strength characteristics, while preserving a high level of plasticity, which is due to the existence of two ensembles of dispersed particles: an ensemble of intermetallics η'-($MgZn_2$) phase and $Al_3(Sc_{1-x}Zr_x)$ particles coherently bound to the matrix.

3. It is shown that, in the Al–8.0Zn–2.6Mg–2.3Cu–0.15Zr–0.3Sc–0.2Hf alloy, the composition of nanosized hardening particles based on the Al_3Sc intermetallic also includes zirconium and hafnium.

4. The structure of the investigated rods alloys after T6 treatment was studied, and it was shown that Sc + Zr doping of the base alloy with the addition of Hf stabilizes the structural state of the alloy, and, after annealing at 80°C, there are no significant changes in the size and distribution of hardening particles. This allowed obtaining the following mechanical characteristics at 80°C after prolonged holding at 80°C: $Y_S = 636$ MPa, $U_{TS} = 731$ MPa, $E_l = 14.5\%$ (which is 30% higher than the U_{TS} of the base alloy).

REFERENCES

1. B. Zhou, B. Liu, and S. Zhang, *Metals*, **11**, Iss. 5: 718 (2021).
2. M. Ashjari and A. J. Feizi, *Mater. Sci. Eng. Int. J.*, **2**, Iss. 2: 49 (2018).
3. Yu-guo Liao, Xiao-qi Han, Miao-xia Zeng, and Man Jin, *Mater. Design*, **66**, Pt. B: 581 (2015).
4. Yu. V. Milman, *Vliyanie Skandiya na Strukturu, Mekhanicheskie Svoistva i Soprotivlenie Korrozii Splavov Alyuminiya* [The Influence of Scandium on the Structure, Mechanical Properties and Corrosion Resistance of Aluminium Alloys] (Kiev: Akademperiodika: 2003), vol. **1**, p. 335 (in Russian).
5. X. Dai, C. Xia, X. Peng, and K. Ma, *J. Univ. Sci. Technol. B*, **15**, Iss. 3: 276 (2008).
6. Yu. V. Milman, A. I. Sirko, D. V. Lotsko, O. N. Senkov, and D. B. Miracle, *Mater. Sci. Forum*, **396–402**: 1217 (2002).
7. D. V. Lotsko, Yu. V. Milman, N. A. Efimov, A. P. Rachek, and L. N. Trofimova, *Met. Phys. Adv. Tech.*, **19**, Iss. 6: 783 (2001).
8. Yu. V. Milman, D. V. Lotsko, N. A. Iefimov, N. M. Mordovets, A. P. Rachek, and L. N. Trofimova, *Metallofiz. Noveishie Tekhnol.*, **26**, No. 10: 1363 (2004) (in Russian).
9. E. Lavernia, G. Rai, and N. J. Grant, *Mater. Sci. Eng.*, **79**, Iss. 2: 211 (1986).
10. Y. Dai, L. Yan, and J. Hao, *Mater.*, **15**, Iss. 3: 1216 (2022).
11. L. F. Mondolfo, *Aluminum Alloys: Structure and Properties* (London–Boston: Butterworths Publisher: 1976), p. 11.
12. U. Tenzler and E. Cyrener, *Aluminium*, **75**, No. 6: 524 (1999).
13. G. Sha and A. Cerezo, *Surf. Interface Analysis*, **36**, Iss. 5–6: 564 (2004).
14. M. F. Ashby and L. M. Brown, *Phil. Mag.*, **8**, No. 91: 1083 (1963).
15. Yu. V. Milman, *Metallofiz. Noveishie Tekhnol.*, **27**, No. 1: 59 (2005) (in Russian).